Kronig–Penney model with the tail-cancellation method

Subodha Mishra and S. Satpathy[a)]
Department of Physics & Astronomy, University of Missouri, Columbia, Missouri 65211

(Received 14 July 2000; accepted 24 August 2000)

The Kronig–Penney model of an electron moving in a periodic potential is solved by the so-called tail-cancellation method. The problem also serves as a simple illustration of the tail-cancellation method itself.
[DOI: 10.1119/1.1326074]

The Kronig–Penney model serves to illustrate the formation of energy bands in a periodic solid and appears as a pedagogical example in many textbooks in elementary solid state physics. The model is generally solved either by matching the boundary conditions for the wave functions at the cell boundaries,[1] by a plane-wave expansion of the wave function in the reciprocal lattice space,[2] or even by the somewhat more involved T-matrix method.[3]

In this note, we point out that perhaps the simplest way of solving the problem is by using the tail-cancellation condition, which has been used extensively in the solution of the band structure problem in realistic solids.[4] The solution therefore serves as a simple illustration of the tail-cancellation method as well.

The Schrödinger equation for a one-dimensional solid is

$$-\frac{\hbar^2}{2m}\frac{d^2\Psi(x)}{dx^2}+U(x)\Psi(x)=E\Psi(x), \tag{1}$$

where the potential is periodic with lattice constant a:

$$U(x)=\sum_{n=-\infty}^{\infty} V(x-na). \tag{2}$$

Consider first a single potential well, where the potential is $V(x)$ in the central cell, $-a/2\leqslant x\leqslant a/2$, and zero elsewhere. Once we find a solution $\phi(x)$ to this potential for a given energy E, the wave function for the solid $\Psi(x)$ may be constructed by taking a linear superposition of such functions centered in different cells, with the coefficients given by the Bloch theorem, i.e.,

$$\Psi(x)=\sum_n e^{ikna}\phi(x-na), \tag{3}$$

where k is the Bloch momentum. Now, since $\phi(x)$ already is a solution of the Schrödinger equation in the central cell, the ''tails'' of the functions $\phi(x-na)$ coming from other cells must interfere destructively inside the central cell (and hence inside any other cell). Thus we have the condition

$$\sum_{n\neq 0} e^{ikna}\phi(x-na)=0 \tag{4}$$

for all values of x in the central cell. This is the so-called ''tail-cancellation'' condition. The problem therefore boils down to finding the solution $\phi(x)$ for a given energy for a single potential well and then applying the tail-cancellation condition. If the condition can be satisfied then we have a solution for that energy, otherwise not.

We now apply the method to the Kronig–Penney model. For a single potential well, the most general solution of the Schrödinger equation for the energy E is given by

$$\phi(x)=A\phi_1(x)+B\phi_2(x), \tag{5}$$

where ϕ_1 and ϕ_2 are the two independent solutions with energy E. These solutions extend in all space and for the case of the one-dimensional potential may be written in terms of the transmission and reflection coefficients:

$$\begin{aligned}\phi_1(x)&=e^{iKx}+re^{-iKx}, \quad x\leqslant -a/2\\ &=te^{iKx}, \quad x\geqslant a/2\end{aligned} \tag{6}$$

and

$$\begin{aligned}\phi_2(x)&=te^{-iKx}, \quad x\leqslant -a/2\\ &=e^{-iKx}+re^{iKx}, \quad x\geqslant a/2,\end{aligned} \tag{7}$$

where $\hbar^2K^2/2m=E$. Notice that the above wave functions are simply the ''tails''—we don't really care at this point how the wave function looks inside the cell itself, i.e., for $|x|\leqslant a/2$. Once the energy is obtained, the wave function inside the cell (and hence everywhere) may be obtained by integrating the Schrödinger equation.

Substituting the expression for $\phi(x)$ from Eqs. (5) to (7) in the tail-cancellation condition Eq. (4), equating the coefficients of $e^{\pm iKx}$ to zero, and eliminating A and B, we obtain the following condition:

$$(r^2-t^2)f_+f_- -t(f_+f_-^*+f_+^*f_-)-f_+^*f_-^*=0, \tag{8}$$

where $f_\pm\equiv f(K\pm k)$ and $f(\kappa)=\Sigma_{n=1}^{\infty}e^{i\kappa na}$.

The last sum is over a series of oscillating terms. The oscillation can be traced to the fact that the plane-wave-like tails in Eqs. (6) and (7) continue undamped to infinity. If we keep a finite number of terms N in the summation, then the second term in the numerator of the result $f(\kappa)=(e^{i\kappa a}-e^{i\kappa(N+1)a})/(1-e^{i\kappa a})$ oscillates rapidly between -1 and $+1$ as $N\to\infty$ with the average value zero. It turns out that taking this average value yields the correct answer for the problem at hand.

A more careful way of evaluating the sum is to take the limit

$$f(\kappa)=\lim_{N\to\infty,\mu\to 0}\sum_{n=1}^{N} e^{(i\kappa-\mu)na}=\frac{e^{i\kappa a}}{1-e^{i\kappa a}}, \tag{9}$$

where the limit has been taken in such a way that $\mu a \ll 1$ and $\mu N a \gg 1$. Physically this corresponds to a small damping term $e^{-\mu|x|}$ in the two basis functions Eqs. (6) and (7) such that the amplitudes of the plane-wave tails damp out at infinity but do not change appreciably over the length of a unit cell.

We now write the transmission coefficient in terms of the phase-shift η, $t=|t|e^{i\eta}$, so that the reflection coefficient has the well-known general form $r=\pm i|r|e^{i\eta}$. Substituting Eq. (9) into Eq. (8) we get the desired result

$$\frac{\cos(Ka+\eta)}{|t|}=\cos ka. \tag{10}$$

This is the standard transcendental equation for the model,[5] which we derived here from the tail-cancellation condition.

For a periodic array of δ functions $V(x)=g\,\delta(x)$, Eq. (10) takes the form

$$\left(\frac{P}{Ka}\right)\sin Ka+\cos Ka=\cos ka, \tag{11}$$

where the well-known result, $|t|=\cos\eta$ and $\tan\eta=-mg/\hbar^2k$, for the transmission coefficient of the delta-function potential has been used and $P\equiv mag/\hbar^2$.

In summary, we have shown how the tail-cancellation condition can be applied to the solution of the Kronig–Penney model.

[a]Electronic mail: satpathys@missouri.edu

[1]C. Kittel, *Introduction to Solid State Physics* (Wiley, New York, 1996), 7th ed., p. 180.
[2]S. Singh, ''Kronig–Penney Model in Reciprocal Lattice Space,'' Am. J. Phys. **51**, 179 (1983).
[3]W. J. Titus, ''Solutions of the Kronig–Penney Models by the T-Matrix Method,'' Am. J. Phys. **41**, 512–516 (1973).
[4]See, for example, H. L. Skriver, *The LMTO Method* (Springer, New York, 1983).
[5]N. W. Ashcroft and N. D. Mermin, *Solid State Physics* (Saunders, Philadelphia, 1976), p. 148.

Comment on ''A simple demonstration of the Alford–Gold effect using a diode laser and optical fibers,'' by L. Basano and P. Ottonello [Am. J. Phys. 68 (4), 325–328 (2000)]

A. C. de la Torre[a]
Departamento de Física, Universidad Nacional de Mar del Plata, Funes 3350, 7600 Mar del Plata, Argentina

(Received 7 July 2000; accepted 21 August 2000)

[DOI: 10.1119/1.1326073]

An experimental demonstration[1] has been presented in this journal[2] using a diode laser, two optical fibers, a photodiode, and a wave analyzer. This demonstration is very simple and has the didactic value of clearly presenting important optical concepts. In this note I propose a simplification of the experimental apparatus that, as a further advantage, should allow the observation of the Alford–Gold effect in a more interesting way.

In their experimental demonstration, L. Basano and P. Ottonello use *two* optical fibers although the same can be achieved with just *one* optical fiber, as is schematically shown in Fig. 1. In this case, one of the beams goes directly to the photodiode and the other, extracted with the beam splitter BS1, is retarded in an optical fiber before being directed, with a beam splitter BS2, to the photodiode (I have omitted in the drawing possible positioning of lenses). In the space between the two beam splitters, additional beam splitters, or a partially reflecting mirror, can be placed if it is desired to compensate for the transmission losses of the other beam. This setup amounts to a slight simplification of the apparatus but is essentially the same experiment. A real improvement of the experiment is obtained with a further modification of the setup. For this, we can eliminate the second beam splitter (BS2) and place the end of the optical fiber at the *top side* of (BS1) in order to feed the reflected part into the photodiode. Notice, however, that the *transmitted* part can make (with proper alignment) a second turn along the optic fiber with the corresponding time delay 2τ. This would cause second-order dips in the spectral analysis, separated by half of the separation of the first-order dips. Perhaps higher order dips can also be observed.

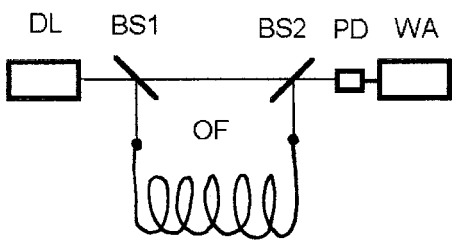

Fig. 1. Experimental setup. DL=diode laser; BS1, BS2=beam splitters; PD=photodiode; WA=wave analyzer; OF=optic fiber.

[a]Electronic mail: dltorre@mdp.edu.ar

[1]A. P. Alford and A. Gold, ''Laboratory measurement of the velocity of light,'' Am. J. Phys. **26**, 481–484 (1958).
[2]L. Basano and P. Ottonello, ''A simple demonstration of the Alford–Gold effect using a diode laser and optical fibers,'' Am. J. Phys. **68**, 325–328 (2000).

Comment on "Bound states of a uniform spherical charge distribution—revisited!," by Brian C. Tiburzi and Barry R. Holstein [Am. J. Phys. 68 (7), 640–648 (2000)]

Frank Rioux[a)]
Department of Chemistry, St. John's University/College of St. Benedict, St. Joseph, Minnesota 56374

(Received 24 July 2000; accepted 9 August 2000)

[DOI: 10.1119/1.1326075]

I would like to suggest an alternative solution to the interesting finite-nucleus problem recently discussed by Tiburzi and Holstein,[1] and previously by Zablotney.[2] While these authors solve this problem by matching interior and exterior solutions to Schrödinger's equation at the nuclear radius, it is also possible to obtain solutions by direct numerical integration of the radial equation in a single integration procedure.[3]

Figure 1, which is a MATHCAD 5.0 worksheet, demonstrates how easily this can be accomplished. MATHCAD's graphical interface displays the calculation clearly in its entirety, unencumbered by arcane programming language. The figure shows the numerical calculation for the 1*s* state of muonic lead, which is in agreement with the results of Ref. 1. Good agreement is also obtained for the higher muonic states of lead.

The numerical integration approach used here requires an initial energy guess to generate a trial solution. This seed value can be provided by the point-nucleus expression for the energy—$E_n = -\mu Z^2/2n^2$. This initial energy value will generate a wave function which does not satisfy the right-hand boundary condition because it is much too low for a

Integration grid, integration limits, reduced mass, angular momentum, nuclear charge, and nuclear radius:

$n := 600 \quad Rmin := 0 \quad Rmax := .0008 \quad \Delta := \frac{Rmax - Rmin}{n} \quad \mu := 206.771 \quad L := 0 \quad Z := 82 \quad Rn := 1.343 \cdot 10^{-4}$

Integration algorithm begins: $R_0 := if(L > 0, 0, 1) \quad R_1 := .99 \quad r_1 := Rmin + \Delta$

$i := 2, 3 .. n \quad r_i := Rmin + i \cdot \Delta \quad V_{i-1} := if\left[r_{i-1} \le Rn, \frac{-Z}{Rn} \cdot \left[\frac{3}{2} - \frac{(r_{i-1})^2}{2 \cdot Rn^2}\right], \frac{-Z}{r_{i-1}}\right]$

$$R_i := \frac{\left[2 \cdot R_{i-1} + \left[\frac{L \cdot (L+1)}{(r_{i-1})^2} - 2 \cdot \mu \cdot (E - V_{i-1})\right] \cdot R_{i-1} \cdot \Delta^2 - \left(1 - \frac{\Delta}{r_{i-1}}\right) \cdot R_{i-2}\right]}{\left(1 + \frac{\Delta}{r_{i-1}}\right)}$$

Enter energy guess: $E := -382680$ **Convert energy to eV:** $E \cdot 27.2114 = -1.0413 \cdot 10^7$

Normalize wave function: $i := 0, 2 .. n - 2 \quad N := \left[4 \cdot \pi \cdot \left[\sum_i \left[(r_i \cdot R_i)^2 + 4 \cdot (r_{i+1} \cdot R_{i+1})^2 + (r_{i+2} \cdot R_{i+2})^2\right] \cdot \frac{\Delta}{3}\right]\right]^{-\frac{1}{2}}$

Plot radial wavefunction: $i := 0 .. n \quad R_i := N \cdot R_i$

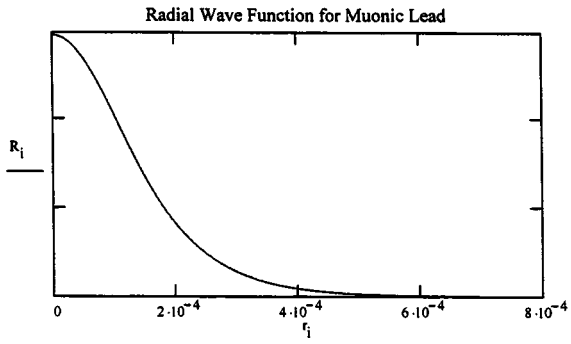

Fig. 1. Numerical integration of the radial equation for the 1*s* state of muonic lead using parameters provided in Ref. 1.

muonic system in which the muon spends considerable time within the nucleus. The energy value is adjusted upward until the right-hand boundary condition is satisfied (see Fig. 1). The large difference between the seed value and the final energy value (-18.916 vs -10.413 MeV for the $1s$ state) demonstrates the significance of the finite size of the nucleus for muonic atoms.

The fine structure corrections outlined by Tiburzi and Holstein [their Eqs. (16)–(18)] can be easily added to the MATHCAD worksheet (omitted here for the sake of brevity), using traditional numerical algorithms, so that a thorough comparison of theory and experiment can be made.

[a]Electronic mail: frioux@csbsju.edu

[1]B. C. Tiburzi and B. R. Holstein, ''Bound states of a uniform spherical charge distribution-revisited!,'' Am. J. Phys. **68**, 640–648 (2000).
[2]J. Zablotney, ''Energy levels of a charged particle in the field of spherically symmetric uniform charge distribution,'' Am. J. Phys. **43**, 168–172 (1975).
[3]F. Rioux, ''Direct numerical integration of the radial equation,'' Am. J. Phys. **59**, 474–475 (1991).

Comment on ''Charge density on a thin straight wire, revisited,'' by J. D. Jackson [Am. J. Phys. 68 (9), 789–799 (2000)]

O. F. de Alcantara Bonfim and David Griffiths[a)]
Reed College, Portland, Oregon 97202

(Received 5 September 2000; accepted 12 September 2000)

[DOI: 10.1119/1.1326076]

Jackson's paper[1] supports an emerging consensus[2] that the linear charge density on a conducting wire is uniform, in the zero radius limit. This is easily proved for the special case of an ellipsoid, but Jackson demonstrates that it holds regardless of shape. This conclusion is so counterintuitive that we decided to reexamine the original numerical studies,[3] based on discrete charge distributions, that appeared to confirm the more plausible hypothesis that the charge accumulates preferentially near the ends.

We place N charges at equal spacing on the interval $0<x\leqslant 1$:

$$\begin{aligned} &q_1 \quad \text{at } x_1=1/N,\\ &q_2 \quad \text{at } x_2=2/N,\\ &\cdots\\ &q_n \quad \text{at } x_n=n/N,\\ &\cdots\\ &q_N \quad \text{at } x_N=1 \end{aligned} \tag{1}$$

(and equal charges at the corresponding points on $-1\leqslant x<0$), together with a single charge q_0 at $x_0=0$. We then adjust the charges so that the Coulomb force on each of them except q_N (which is subject to an extra confining force) is zero:

$$\sum_{j=1}^{N}\frac{q_j}{(n+j)^2}+\frac{q_0}{n^2}+\sum_{j=1}^{n-1}\frac{q_j}{(n-j)^2}-\sum_{j=n+1}^{N}\frac{q_j}{(j-n)^2} =0 \quad (n=1,2,\ldots,N-1), \tag{2}$$

subject to the constraint

$$q_0+2\sum_{n=1}^{N}q_n=1 \tag{3}$$

(the scaled total charge on the wire). This does not determine the charge at the center—the force on q_0 is automatically zero, by symmetry. To ensure continuity we choose $q_0=q_1$. What remains is a set of N linear equations for the N unknown charges.

Griffiths and Li[2] solved this system numerically for N up to 100, and persuaded themselves that the linear charge density was approaching a nontrivial limiting form—fairly flat in the center, but with spikes at the ends ($x=\pm 1$). They were seduced by extraordinarily slow convergence as N

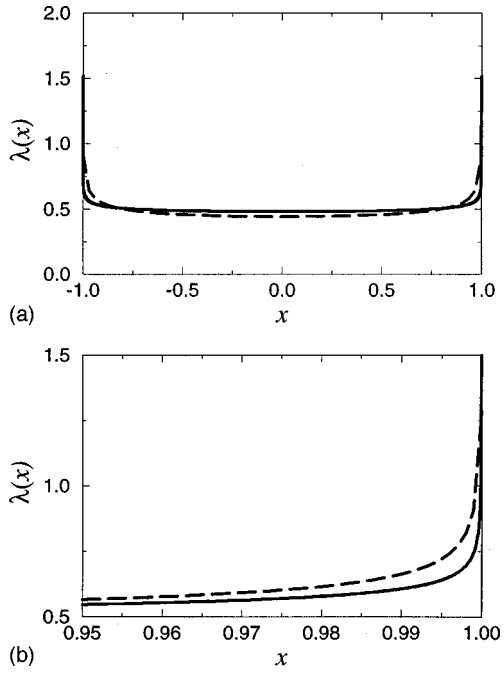

Fig. 1. Linear charge density on a needle, as a function of position. The calculation was done using $2N+1$ point charges equally spaced on the interval from -1 to $+1$, and requiring that the net force on each charge (except the end two) vanish. The total charge on the needle is 1. (a) Solid line: $N=16\,384$; dashed line: $N=32$. (b) Expanded view of the right end; this time the dashed line is $N=1024$.

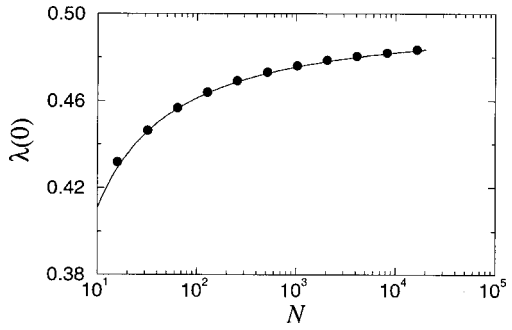

Fig. 2. Charge density at the center of the needle, as a function of N. Dots represent the numerical results. The solid line is the best fit of the form $\lambda(0)=P_1+P_2/\ln N+P_3/(\ln N)^2$ (for N ranging from 32 to 16 384), which occurs for $P_1=0.500$, $P_2=-0.152$, and $P_3=-0.123$. Evidently $\lambda(0)$ approaches the uniform density value of 0.5, as N increases.

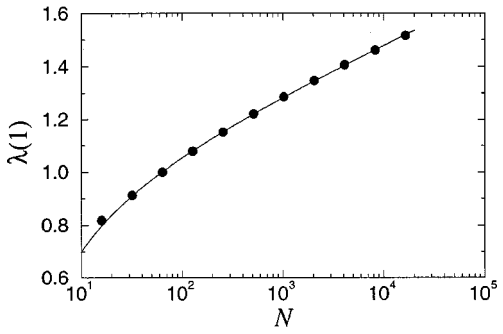

Fig. 3. Charge density at the ends of the needle ($x=\pm1$), as a function of N. Dots represent the numerical results. The solid line is the best fit of the form $\lambda(1)=[Q_1+Q_2/\ln N+Q_3/(\ln N)^2]\ln N$, which occurs for $Q_1=0.0719$, $Q_2=0.912$, and $Q_3=-0.874$. Evidently $\lambda(\pm1)$ diverges as N increases.

$\rightarrow\infty$, as we can see from Fig. 1, which extends the calculation out to $N=16\,384$: As N increases, the charge density approaches 1/2, except at the very ends, which occupy a decreasing portion of the length and contain a diminishing fraction of the total charge.

In Fig. 2 we plot the charge density at the center ($\lambda(0)=Nq_0$) as a function of N, to demonstrate the (painfully slow) approach to 0.5. Jackson shows that the natural expansion parameter is Λ^{-1}, where $\Lambda\equiv\ln(4c^2/a^2)$, with $2c$ the length of the wire and a its characteristic ''radius,'' and he suggests that for the discrete model this translates to $\Lambda\sim2\ln N$. In Fig. 2 the solid line is a best fit of the form

$$\lambda(0)=P_1+\frac{P_2}{\ln N}+\frac{P_3}{(\ln N)^2}; \tag{4}$$

for our data (with N ranging from 32 to 16 384) $P_1=0.500$, $P_2=-0.152$, and $P_3=-0.123$.

In Fig. 3 we plot the charge density at the ends of the wire ($\lambda(1)=Nq_N$), as a function of N. It seems clear that this quantity increases without limit—in fact, our data are well represented by the functional form

$$\lambda(1)=\left[Q_1+\frac{Q_2}{\ln N}+\frac{Q_3}{(\ln N)^2}\right]\ln N, \tag{5}$$

with $Q_1=0.0719$, $Q_2=0.912$, and $Q_3=-0.874$ (solid line). Nevertheless, these ''rabbit ears'' in $\lambda(x)$ are of decreasing significance as $N\rightarrow\infty$, in the sense that they occupy a diminishing portion of the total length and contain a smaller and smaller fraction of the total charge.

ACKNOWLEDGMENT

We thank Nicholas Wheeler for illuminating discussions of this problem.

[a]Electronic mail: Griffith@reed.edu

[1]J. D. Jackson, ''Charge density on a thin straight wire, revisited,'' Am. J. Phys. **68**, 789–799 (2000).

[2]R. H. Good, ''Comment on 'Charge density on a conducting needle,' '' Am. J. Phys. **65**, 155–156 (1997); Mark Andrews, ''Equilibrium charge density on a conducting needle,'' *ibid.* **65**, 846–850 (1997); Nicholas Wheeler, ''Construction and applications of the fractional calculus'' (unpublished).

[3]D. J. Griffiths and Ye Li, ''Charge density on a conducting needle,'' Am. J. Phys. **64**, 706–714 (1996).

PREPARATION?

Gibbs began his lectures on thermodynamics with the Carnot cycle, which he always got wrong. After getting thoroughly mixed up he concluded the first lecture with an apology, and in the second lecture he gave it letter perfect. It was in this way he introduced entropy, rather than in the formal way in the ''Heterogeneous Substances''.

E. B. Wilson, a student of J. Willard Gibbs, as quoted by Clifford Truesdell in J. Serrin (editor), *New Perspectives in Thermodynamics* (Springer, New York, 1986), p. 107.